



# Conformational turn triggers regio-selectivity in the bioactivation of thiophene-contained compounds mediated by cytochrome P450

Chun-Zhi Ai<sup>1,2</sup> · Yong Liu<sup>3</sup> · Du-Chu Chen<sup>1,2</sup> · Yasmeen Saeed<sup>1,2</sup> · Yi-Zhou Jiang<sup>1</sup>

Received: 5 April 2019 / Accepted: 24 July 2019 / Published online: 10 September 2019  
© Society for Biological Inorganic Chemistry (SBIC) 2019

## Abstract

In the present work, we performed Density Functional Theory calculations to explore the bioactivation mechanism of thiophene-containing molecules mediated by P450s. For this purpose, relatively large size compounds, 2,5-diaminothiophene derivatives were selected particularly for this investigation. Here we found the successive regio-selectivity triggered by conformational turn played a significant role in the occurrence of bioactivation. 2,5-Diaminothiophene was oxidized to a 2,5-diimine thiophene-reactive intermediate by Compound I (Cpd I) through successive activations of two N–H bonds (H3–N11 and H1–N6). This reaction exhibited three special characteristics: (1) self-controlled regio-selectivity during the oxidation process. There was a large scale of conformational turn in the abstraction of the first H atom which triggers the selection of the second H for abstraction. (2) Proton-shuttle mechanism. In high spin (HS) state, proton-shuttle mechanism was observed for the abstraction of the second H atom. (3) Spin-selective manner. In protein environment, the energy barrier in HS state was much lower than that in low spin state. The novel proposed bioactivation mechanism of 2,5-diaminothiophene compounds can help us in rational design of thiophene-contained drugs avoiding the occurrence of bioactivation.

**Keywords** DFT calculations · Cytochrome P450 · Self-controlled regio-selectivity · Bioactivation mechanism · Thiophene-contained compound

## Introduction

Idiosyncratic adverse drug reactions (IADRs) have been attributed as the major cause of drug withdrawn from the market. Among these, the most common IADRs, drug-induced liver injury (DILI), accounts for 50% of the acute liver failure cases [1]. Recently published epidemiologic data demonstrate that DILI occurs with an annual incidence

of about 14–19 per 100,000 inhabitants [2]. In most instances, the metabolic bioactivation of drug into chemically reactive metabolites has been generally believed to be responsible for the occurrence of IADRs. This is because the reactive metabolite has the ability to covalently modify cellular macromolecules, i.e., proteins, lipids, and nucleic acids, resulting in protein dysfunction, lipid peroxidation, DNA damage, and oxidative stress [3, 4]. It has been elucidated that mammalian cytochrome P450s are involved in the majority of oxidations of electrophiles [5–8].

Some of certain functional groups, i.e., the acetylenes, thiophenes, arylamines, quinones, and numerous others have been reported to predispose the molecule to be metabolized by particular P450 enzymes that account for the generation of reactive metabolites [9]. At same time they are often effective pharmacophores in drug discovery, like thiophene rings, and represents as attractive isosteric replacements for improved potency and selective SAR [10]. Actually, about 50% of the 200 most frequently prescribed drugs in the US possess more than one structural alert [11, 12]. However, most of them do not show IADRs. A wide concern arises whether compounds containing these

**Electronic supplementary material** The online version of this article (<https://doi.org/10.1007/s00775-019-01699-6>) contains supplementary material, which is available to authorized users.

✉ Yi-Zhou Jiang  
jiangyz@szu.edu.cn

<sup>1</sup> Institute for Advanced Study, Shenzhen University, Shenzhen, Guangdong, China

<sup>2</sup> Key Laboratory of Optoelectronic Devices and Systems of Ministry of Education and Guangdong Province, College of Optoelectronic Engineering, Shenzhen University, Shenzhen, Guangdong, China

<sup>3</sup> School of Life Science and Medicine, Dalian University of Technology, Panjin, Liaoning, China

functional groups will be bioactivated into reactive intermediates, and what kind of structures will avoid the metabolic bioactivation.

Thiophene group is a useful isosteric building block that can improve pharmacokinetic and pharmacodynamic properties of a drug [10, 13]. Compounds containing thiophene always exhibit varieties of pharmacological efficacies, such as nematocidal, antifungal, antiviral effects, etc. [14–16]. Meanwhile, it is a structural alert. In the past decades, some thiophene-containing drugs such as tienilic acid (TA), suprofen, methapyrilene, etc., have been reported of IADRs [17–21], which has been associated with their P450-mediated oxidative metabolic activation [22–24]. Generally, thiophenes can be biotransformed into three kinds of electrophilic intermediates, e.g., thiophene *S*-oxides, thiophene epoxides, and sulfenic acids through oxidative metabolism of P450s [12, 25–27]. Hu et al. investigated the P450s-mediated metabolic activation of an anti-inflammatory agent, 1-(3-carbamoyl-5-(2,3,5-trichlorobenzamido)thiophen-2-yl) urea and its derivatives through in vitro method [28]. They proposed a novel mechanism, the 2,5-diaminothiophene moiety undergoes oxidation to a 2,5-diimine thiophene-reactive intermediate [28]. How does this reaction occur? Can this bioactivation be avoided?

P450s accomplish the most important oxidation reactions through the catalytic cycle. In the cycle, the putative high-valent iron (IV)-oxo porphyrin radical cation species called Compound I (Cpd I) was usually considered to be responsible for the oxidation with the incorporation of an oxygen atom into organic substrates, such as C–H hydroxylation, C=C epoxidation and sulfoxidation et al. [29, 30]. Cpd I and its surrounding amino acids constitute the active pocket for the substrate to situate in. The substrate selectivity is, thus, tightly associated with its binding into the pocket that directs the eventual catalysis.

The selectivity of oxidation is determined by many factors, such as the nature of rate-limiting step, the binding interaction-related steric and electrostatic effects, as well as the catalysis-related intrinsic electronic reactivity [31]. In most cases, it is more influenced by the interaction-related factors regarding the substrate binding site of individual cytochromes P450, and for this reason, methods like molecular docking and molecular dynamics simulation are widely employed to mimic the stereo- and regio-selectivity. On the other hand, very few studies are available on the regio-selectivity determined by the oxidation process. Previous studies on regio-selectivity in the oxidation mediated by P450s were explored in terms of the selectivity of allylic hydroxylation or double bond for small molecules like cyclohexene, propene and DHA, etc. [32–34]. What these investigations focused on was the first-attack regio-selectivity by Cpd I. However, it has been rarely investigated that: how two or more regio-sites could be selected for successive reaction

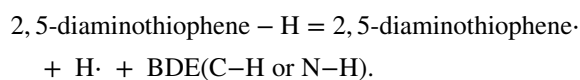
steps during the oxidation process? Particularly, can such selectivity take place when the two sites are far away from each other for some relative big compounds?

The present study was designed to explore the successive regio-selectivity of two sites in the bioactivation of thiophene compound with the iron (IV)-oxo species, Cpd I. 2,5-diaminothiophene derivatives were selected particularly and Density Functional Theory (DFT) method was employed to mimic the catalytic process of bioactivation along which we can find out how successive regio-selectivity occurred during oxidation without the aid of amino acids that was critical for the formation of the active intermediate. The objective of present study was to specify the underlying bioactivation mechanism of 2,5-diaminothiophene that will shed light to the avoidance of the occurrence of bioactivation in the discovery of thiophene-containing drugs.

## Method and model

Six 2,5-diaminothiophene derivatives were concerned in the context, which were labeled as no. 1–6. Molecule 1 was selected for the full analysis of the reaction mechanism and the others were used to assess the role of conformational turn in the occurrence of bioactivation.

We first computed the bond dissociation energy (BDE) of C–H or N–H bonds of Molecule 1 to assess which regio-site was first preferred by Cpd I. The H-abstraction energy of thiophene-containing compound was studied by computing the C–H and N–H bond dissociation energy (BDE) at the UB3LYP/6-311+G\* level to assess which regio can be added to Cpd I first. The BDE was computed as the difference of 2,5-diaminothiophene-H energy and the energy of radicals (2,5-diaminothiophene· and H·). The energy of 2,5-diaminothiophene· moiety and 2,5-diaminothiophene all corresponded to their final optimized geometries [31].



Subsequently, we performed DFT computations to mimic the catalytic pathways of 2,5-diaminothiophene bioactivated by P450s. The DFT computation used spin-unrestricted hybrid density functional UB3LYP which has proved to be accurate in Cpd I-mediated reactions [35, 36]. Two basis sets was used: (1) the LACVP basis set on iron, and the 6-31G basis set on the remaining atoms (BS-I in brief) for geometry optimization, and (2) the LACV3P+\* basis set on iron, SDD on chlorine, and the 6-311+G\* basis set on all the other atoms (BS-II) for single-point energy calculations. We evaluated the bioactivation reaction in gas phase and non-polar enzymatic environment, respectively. Polarizable continuum model (PCM) solvation model was employed to

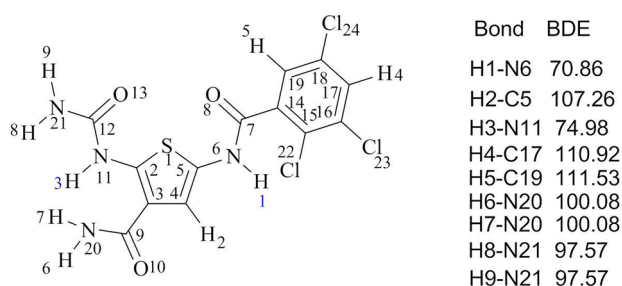


**Fig. 1** Molecular structure, numbering, and the BDE (in kcal mol<sup>-1</sup>) of C–H or N–H of 2,5-diaminothiophene Molecule 1

simulate the effect of polarization by the electric field, where a dielectric constant of  $\epsilon=5.7$  was set for the protein environment [37, 38]. The transition state was optimized and then verified by intrinsic reaction coordinate (IRC) calculations that connected the reactants and products. Mulliken population analysis was carried out to analyze the charge and spin populations of the final energy calculations [39].

Cpd I was modeled as an iron-oxo-porphyrin complex,  $\text{Fe}^{4+}\text{O}^{2-}(\text{C}_{20}\text{N}_4\text{H}_{12})^-(\text{SH})^-$ , without any side chains but with a proximal thiolate ligand [35, 40]. The ground state of Cpd I show a quasi-degenerate pair of triradicaloid states, which gives rise to two close-lying electronic states, e.g., doublet and quartet spin states or referred as the low-spin (LS) and high-spin (HS) states [41]. In the present investigation, we optimized the geometries in LS and HS states, respectively. We used 2 and 4 to denote the LS and the HS species in the context, respectively. Previous study suggested the  $\text{SH}^-$  ligand along with these simple mimics of the environmental effects represents the state of Cpd I in the protein pocket quite well when they were compared with the QM/MM simulations [42]. All of the calculations were performed with Gaussian 09 package distributed upon high-performance computer systems in National Supercomputing Center in Shenzhen, China [43].

## Results and discussion

In present study we first assessed that which regio-site was preferred by Cpd I by computing the BDE of C–H or N–H for Molecule 1. As shown in Fig. 1, the BDEs of N–H, e.g., site N6 and site N11 were much smaller than those of C–H bonds. So we assumed site N6 and site N11 would be preferred by the oxo species. Considering there will be stereo-hindrance effect between the porphyrin ring and thiophene-containing molecule when N6–H1 was appended to the  $\text{Fe}=\text{O}$  moiety, we assumed that site N11–H3 would be preferred first. In this way, an upstanding pose of 2,5-diaminothiophene with H3 in adjacent to  $\text{Fe}=\text{O}$  moiety of Cpd I was prepared as the original conformation for the subsequent

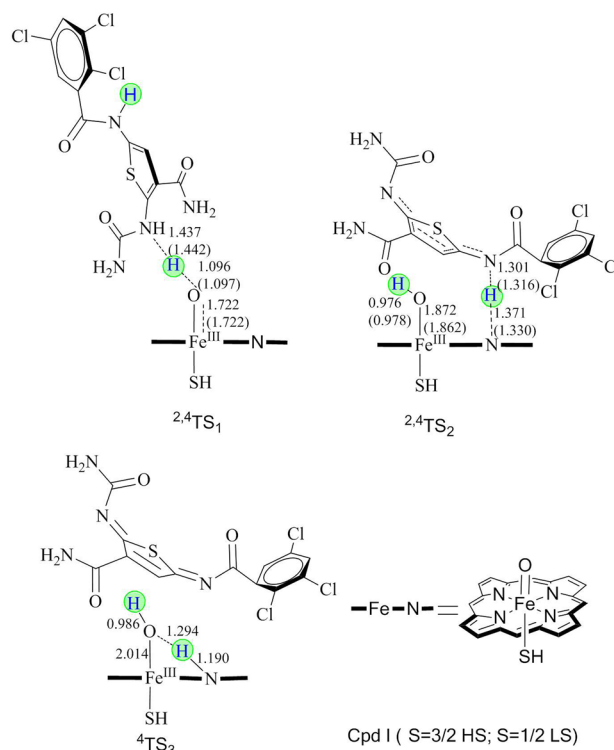


**Fig. 2** Geometries of the transition state in the oxidation process of 2,5-diaminothiophene Molecule 1 mediated by Cpd I. Data out of the parenthesis and in the parenthesis represent bond length (in Å) for the LS and HS states, respectively. 2 and 4 denote the LS and the HS, respectively

optimization. As expected, we obtained the reactant with 2,5-diaminothiophene-upstanding conformation. On these bases, the reaction mechanism of the bioactivation mediated by P450s was explored. We proposed that two H abstraction steps would be needed to form the reactive intermediate: H3 transfers in first step and H1 transfers in second step. The point is how to complete the two H-transferring steps because H1 is a bit far away from H3. Will the two steps occur successively or independently? Will the conformation of the big molecule 2,5-diaminothiophene be turned for regio-selectivity during the catalytic process? With these questions, we tried to search the transition states of H transferring from 2,5-diaminothiophene to Cpd I with DFT method, which was further verified by IRC method.

Both the LS or HS reaction pathway for Molecule 1 were explored. For the H3-transferring step, there was small difference of geometrical change between the two spin states. For the subsequent abstraction of H1, the two spin states demonstrated distinguished reaction paths: i.e., the LS was observed of one step to accomplish the abstraction of H1 whereas the HS was scanned of two successive transition states for H1 transferring. Geometries of transition states were shown in Fig. 2. Geometrical information of other

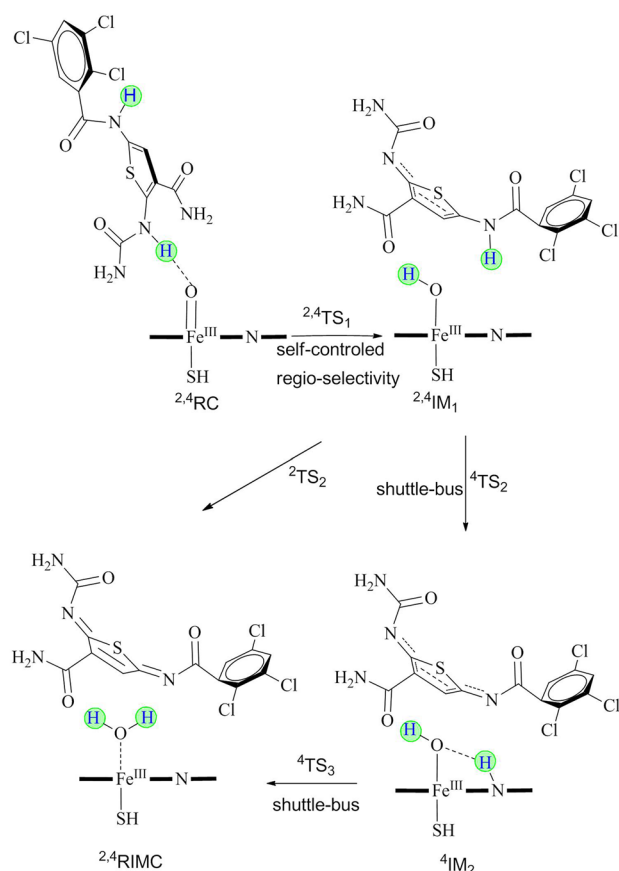


**Fig. 3** The geometrical changes of 2,5-diaminothiophene Molecule 1 along the LS and HS reaction pathways. 2 and 4 denote the LS and the HS state, respectively. Fe–N– represents the porphyrin ring of Cpd I

reaction species can be found in Figure S1 in the Supplementary file. The reaction pathway is summarized in Fig. 3. The H3-transferring transition states ( $^{2,4}TS_1$ ) were obtained with 2,5-diaminothiophene added to the Fe=O moiety of Cpd I in an upstanding style. The two endpoints of the IRC along  $^{2,4}TS_1$  were optimized to find the reactant complexes (RC) and the intermediates (IM). As expected,  $^{2,4}RC$  were in poses with 2,5-diaminothiophene upstanding upon the porphyrin ring, whereas, a conformational turn occurred for 2,5-diaminothiophene after H1 was transferred to Cpd I. As a result,  $^{2,4}IM_1$  were in styles with 2,5-diaminothiophene lying upon the ring. Cpd I accepted H3 to form Fe–O–H moiety, which was referred as Cpd II in some literature [44]. As for  $^{2,4}IM_1$ , the phenyl group of 2,5-diaminothiophene turned approximately parallel to the porphyrin ring and the other moiety was oblique to the ring. H1 was toward the porphyrin ring. For the instance of  $^{2,4}IM_1$ , the distance between H1 and the pyrrol nitrogen of Cpd I was 3.654/3.951 Å and the distance between H1 and =O of Cpd I was 3.534/3.688 Å. The conformational turn means a regio-select behavior can

take place during the oxidation catalysis without the aid of amino acids. There is lack of information about large-scale conformational turn in the oxidation mediated by Cpd I. Our study demonstrates that it was an intrinsic behavior which triggered the regio-selectivity of the second site (H1) to form the reactive intermediate.

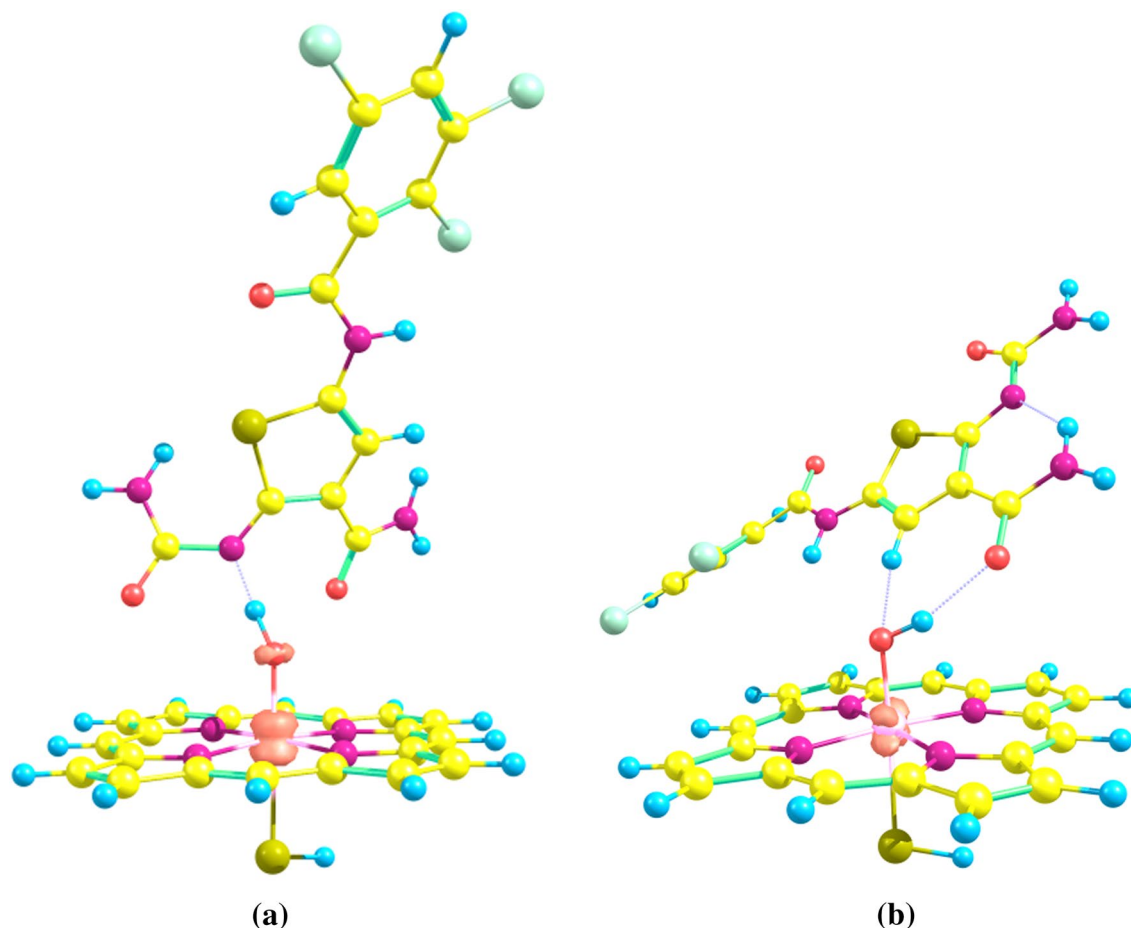
Based on  $^{2,4}IM_1$ , the subsequent LS and HS transition states were obtained by scanning the potential surface. The imaginary frequency vibration suggested that in the conformation of  $^{2,4}TS_2$ , H1 was vibrated towards the nitrogen atom of porphyrin ring. From  $^{2,4}IM_1$  to  $^{2,4}TS_2$ , the bond length of N6–H1 extended to 1.301/1.316 Å, the distance between H1 and the nitrogen of porphyrin was shortened to 1.371/1.330 Å. With the optimization of the endpoints of IRC along with  $^{2,4}TS_2$ , we got different geometries of the subsequent intermediates of LS and HS, respectively. For LS, H<sub>2</sub>O was formed directly with H1 in addition to Fe–O–H<sub>3</sub> moiety, and F–O bond was dissociated. As a result of losing two hydrogen (H3 and H1), the reactive intermediate complex ( $^2RIMC$ ), 2,5-diimine thiophene with the resting state of porphyrin, was formed concertedly. Whereas, the HS demonstrated a distinct pathway: H1 transferred like a shuttle. Leaving N6, H1 first arrived in the nitrogen of the porphyrin to form an N-protonated complex ( $^4IM_2$ ), then it transferred to Fe–O–H moiety via  $^4TS_3$  to form H<sub>2</sub>O molecule. With such proton-shuttle transferring process, the complex of 2,5-diimine thiophene reactive intermediate with a resting state of the heme was generated ( $^4RIMC$ ). 2,5-diimine thiophene possesses a macroconjugated moiety, as shown in Fig. 3, and the C4 site will be attacked by nucleophile like GSH to generate the adduct. It can be seen that the abstraction of H3 give rise to a conformational turn that triggered the selectivity of H1 to form the final reactive intermediates. Additionally, in the catalytic cycle of P450s, one molecule of water will re-enter the pocket to restore the resting state of Heme after Cpd I monooxygenates the substrate. During bioactivation of 2,5-diaminothiophene, Cpd I turned to Cpd II by accepting one H atom and then returned to the resting state with the abstraction of another hydrogen atom.

The charge and spin density analysis demonstrated a mixed cationic and radical nature for the H3 and H1-transferring transition states, as illustrated in Table 1. More details are shown in Tables S1–S4 and Figures S2–S5 in the Supplementary file. There were spin and charge transferred to the substrate. As for the LS reaction path, a decreased trend can be observed for the spin densities upon O atom of Cpd I, from 0.86 of  $R_d$  to 0 of  $P_d$ . The transfer from Cpd I to the substrate mainly occurred in the first step of H abstraction. The spin densities upon Fe of Cpd I was relatively equivalent, except for the increase in  $TS_d1$ . As for the HS, the distribution trend of spin densities upon O atom of Cpd I was similar to that of LS path. An obvious increase trend can be seen for the spin densities upon Fe of Cpd I, from 1.15 of



**Table 1** The distribution of group spin density ( $\rho$ ) and charge ( $Q$ ) upon the 2,5-diaminothiophene Molecule 1 moiety in the complex with Cpd I, where 2 and 4 denote the LS and HS state, respectively

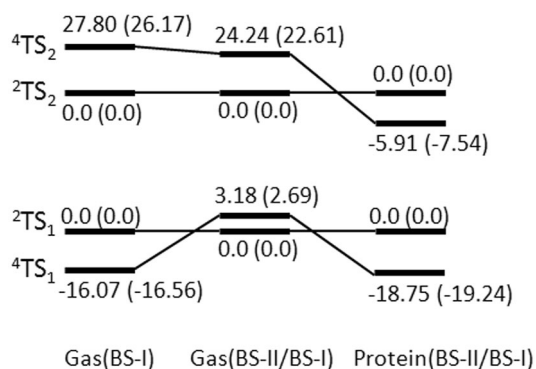
	$R$	$TS_1$	$IM_1$	$TS_2$	$IM_2$	$TS_3$	RIMC
${}^2\rho$	0.00	-0.39	1.00	0.00	-	-	0.00
${}^2Q$	0.02	0.14	0.42	0.85	-	-	0.90
${}^4\rho$	0.01	0.40	1.00	0.37	0.01	0.01	0.00
${}^4Q$	-0.01	0.13	0.49	0.68	0.90	0.93	0.89

**Fig. 4** The spin densities on Fe of  ${}^2TS_1$  (a) and  ${}^2IM_1$  (b). **a**  ${}^2TS_1$  showed a Fe(IV) property; **b**  ${}^2IM_1$  showed a Fe(III) intermediate

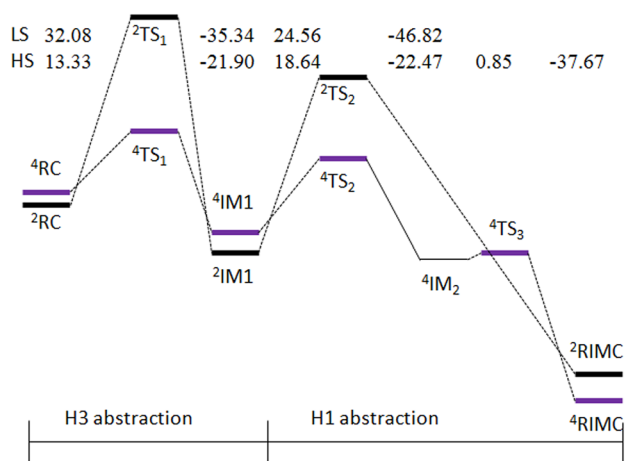
$R_q$  to 3.06 of  $P_q$ , suggesting there can be electronic excitation in the bioactivation process. Specially, the spin density on Fe of  ${}^2IM_1$  shows a Fe(III) intermediate but the  ${}^2TS_1$  shows a Fe(IV) property, as shown in Fig. 4. This suggested that one electron transferred to the iron for  ${}^2IM_1$ .

Figure 5 demonstrates the relative energies of bond activation transition states for the abstraction of H3 and H1 of 2,5-diaminothiophene Molecule 1 under different computational conditions. More detailed energy analysis at different computation level is summarized in Figures S6–S10 and Tables S5, S6 in the Supplementary file. We first discuss the energy profile in gas phase. (1) H3-transferring step. It

was a step that computational level exerted great influence upon the activation barriers of LS and HS. At BS-I level, the activation energy of LS is much higher than that of HS by about 16–17 kcal mol<sup>-1</sup>, and the BS-II/BS-I level computation lowered the activation energy. However, it makes the barrier of HS higher than that of the LS about 2–3 kcal mol<sup>-1</sup>. At BS-II/BS-I level,  ${}^4RC$  needed to overcome a barrier of 15.63 kcal mol<sup>-1</sup> to form  ${}^4TS_1$ . (2) H1-transferring step. Computational level produced smaller influence upon the energy profile of this step. BS-II/BS-I level just lowered the activation energies without any change of the spin effect. Both at the two levels, the activation barriers of HS



**Fig. 5** Relative energies (in kcal mol<sup>-1</sup>) of bond activation transition states for the abstraction of H3 and H1 from 2,5-diaminothiophene Molecule 1 under different computational conditions. For each level we show two energy values: relative energy (out of the parentheses) and relative energy with ZPE corrections (within the parenthesis)



**Fig. 6** Energy profiles (in kcal mol<sup>-1</sup>) of protein environment for the HS and LS bioactivation of 2,5-diaminothiophene Molecule 1 leading to the reactive intermediate, 2,5-diimine thiophene

were much higher than those of LS. In HS, 36.18 kcal mol<sup>-1</sup> of energy was required to accomplish the transfer of H1 at BS-II/BS-I level. (3) proton-shuttle step. This step only occurred in HS, and the energy barrier was negligible (1–4 kcal mol<sup>-1</sup>) at any computational level. For LS, it is hard to predict that which step is rate-determining because the activation barriers of TS<sub>1</sub> and TS<sub>2</sub> were equivalent BS-II/BS-I level; whereas for HS, rate-determining step can be clearly attributed to the second step. Assuming the LS and HS pathways occurred independently on account of slow spin crossover, the LS state could be preferred by the bioactivation of 2,5-diaminothiophene in gas phase.

Here we also investigated the influence of polarizing medium on the energy profile. Figure 6 shows the energy barriers obtained in the protein environment. Either for H3-transferring or H1-transferring step, the barriers of LS

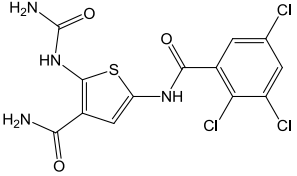
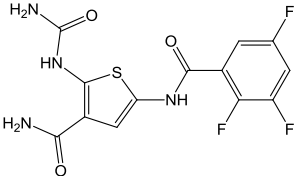
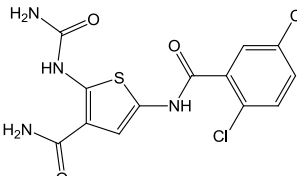
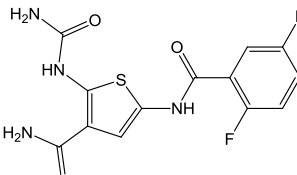
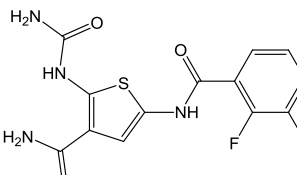
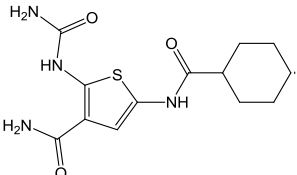
were higher than those of the HS (by 18–19 kcal mol<sup>-1</sup> for TS<sub>1</sub> and 5–6 kcal mol<sup>-1</sup> for TS<sub>2</sub>). In HS, 13.34 kcal mol<sup>-1</sup> was required by <sup>4</sup>RC to cross <sup>4</sup>TS<sub>1</sub> and then 18.65 kcal mol<sup>-1</sup> was taken to form <sup>4</sup>TS<sub>2</sub>. The proton-shuttle process only spared a small energy of 0.85 kcal mol<sup>-1</sup>. Therefore, the RDS of the reaction was the H3-transferring step. The environmental factors can be found to prefer clearly the HS transition states for the abstraction of H3 and H1. Considering the biological system, in human bodies, the reaction will probably be underway in HS.

The parenthetical data in Fig. 5 are relative energies of the transition states for the abstraction of H3 and H1 with zero-point energy (ZPE) correction. More detailed data were shown in Tables S5, S6. Whether for gas phase or protein environment, it can be seen that the ZPE correction brought down all the activation barriers of <sup>2,4</sup>TS<sub>1</sub> and <sup>2,4</sup>TS<sub>2</sub> by 4–5 kcal mol<sup>-1</sup>. The effect ZPE was smaller on <sup>4</sup>TS<sub>3</sub> than the first two step that lowered the barriers by about 2 kcal mol<sup>-1</sup>.

We expect to know whether the conformational turn was a necessary step for the occurrence of the bioactivation. Therefore, DFT simulations have been carried out to investigate the of H3-abstraction process for the other five derivatives of 2,5-diaminothiophene at BS-I level. Either LS or HS state was considered for each molecule. Computational results suggested conformations of Molecules 3 and 5 all turned both in LS and HS states, whereas, Molecule 4 did not exhibit any conformational turn either in LS or HS state. Molecules 2 and 6 can be observed of conformational only in LS state. Correspondingly, the experimental result suggests that the percentage of GSH or NAC adducts were relative small for Molecules 2, 4 and 6 [28], as shown in Table 2.

Comparing the bioactivation process of 2,5-diaminothiophene with the previous reported hydroxylation or epoxidation mediated by P450s, the catalysis of bioactivation exhibited its own characteristics. It is not a typical oxidation reaction because no oxygen atom is incorporated into the substrates, instead, two hydrogen atoms were abstracted. The hydroxylation of C–H or epoxidation of C=C is usually associated with one regio-site of the substrate, mostly two adjacent sites [32–34]. However, previous investigations on regio-selectivity were mainly focused on that: which site would be oxidized or which reaction may occur. For 2,5-diaminothiophene, the bioactivation is associated with two far away sites. How these two sites been selected is also an import topic to explore. With the analysis of DFT computational results, we found a conformational turn occurred in the first step of H3 abstraction that triggered the occurrence of the second step of H1 abstraction. Such a turn demonstrated the self-controlled regio-selectivity characteristics of the substrate in the oxidation process without the aid of amino acids. Therefore, we cannot acquire an expected answer if we employed the structure-based method like docking method to test whether the bioactivation will

**Table 2** The occurrence of conformational turn for 2,5-diaminothiophene derivatives and the in vitro detection of metabolic activation in the presence of GSH or NAC

Molecule	Structure	Spin state	Conformational turn	%GSH adduct	%NAC adduct
1		LS HS	Yes Yes	55%	30%
2		LS HS	Yes No	33%	23%
3		LS HS	Yes Yes	57%	76%
4		LS HS	No No	17%	9%
5		LS HS	Yes Yes	21%	13%
6		LS HS	Yes No	11%	N.A.

The in vitro data were cited from literature [28]

occurred or which site will be bioactivated for molecules like 2,5-diaminothiophene. So it can be speculated that the conformational- turn-triggered regio-selectivity is crucial for the bioactivation of 2,5-diaminothiophene derivatives. Perhaps, it will be queried whether such a big molecule can take a conformational turn in the P450s pocket. The experiment performed by Hu et al. demonstrated that the bioactivation of 2,5-diaminothiophene derivate was mainly mediated by

P450 3A4 [28]. The large and flexible active cavity of 3A4 allows the possibility for 2,5-diaminothiophene turned from a upstanding style to a lying one during oxidation [45].

Another characteristic of the reaction was the spin selective manner. Previous theoretical studies revealed a two-state reactivity (TSR) scenario for the hydroxylation mechanism of alkanes [46, 47], which originates in the closely lying triradicaloid states of Cpd I: a HS state and a LS state.

However, it was different for 2,5-diaminothiophene. There existed a large gap of energy barrier between the HS and LS state, for instance, in protein environment the barrier gap between  ${}^2\text{TS}_1$  and  ${}^4\text{TS}_1$  is 18.75 (19.23) kcal mol $^{-1}$  without (or with) ZPE corrections. It is not common for P450s to show relatively higher energy on doublet state energy surface. Li et al. proposed rather similar energy between  ${}^4\text{TS}_\text{H}$  and  ${}^2\text{TS}_\text{H}$  (N–H abstraction) in their research on *N*-hydroxylation of aromatic amines [48]. The relative energy between  ${}^4\text{RC}$  and  ${}^2\text{RC}$  is small but actually the calculated energy indicated that  ${}^2\text{RC}$  is significantly lower in energy than that of  ${}^4\text{RC}$ , as shown in Table S5. That is also the reason of higher relative energy on doublet state. It is worthy of note that membrane environment played a significant role in the alteration of affinity between the heme iron and cytochrome b5, the redox partner of P450s. The addition of b5, as well as the phospholipids can boost the conversion of LS to HS state that is favorable for catalysis [49]. The experimental result provided considerable support for our simulation result that HS reaction pathway in this system is preferred in protein environment. Moreover, the proton-shuttle mechanism was observed in HS state. The H1 abstraction process became much easier and more integral with the proton-shuttle mechanism involved. Proton-shuttle mechanism was first reported in the hydroxylation of aromatic ring, where the proton transferred via the nitrogen of Cpd I to form the hydroxyl group on the aromatic ring [30]. Here, the proton transferred via the nitrogen of porphyrin to form the  $\text{H}_2\text{O}$ . This process drove the heme to return to the resting state that will reenter the new cycle of the catalysis.

Understanding the bioactivation mechanism of 2,5-diaminothiophene we can find the amine groups adjacent to the sulfur atom (C2 and C5) are capable of generating the reactive intermediate. The molecule without amine groups linked to C2 or C5 will avoid the bioactivation mediated by P450s. Hu et al.'s experimental result suggested that none of the 2-amino or 2,4-diaminothiophene derivatives formed GSH conjugates under the same reaction conditions to that of 2,5-diaminothiophene [28]. They speculated on the basis of the in vitro experiment that 2,5-diaminothiophene might be bioactivated into 2,5-diimine thiophene. However, in their work they did not perform further investigation to explore whether the reaction is possible or how the reaction took place. Our theoretical studies further proved their speculations. Moreover, we provided deep mechanism of the bioactivation among which we found the phenomenon of successive region-selectivity for two far away sites of 2,5-diaminothiophene during the oxidation. Our novel proposed mechanism could enable us to rationally design thiophene-containing drugs with the avoidance of bioactivations.

It should also be stressed that cytochrome P450s were transmembrane proteins. The investigation in the current study mainly concerned the soluble domain of P450s.

However, the membrane environment of P450s might exert a lot influence on the folding and stabilized structures, the spin state of the heme, as well as the catalytic mechanism. In the past decades, the useful method to obtain the crystal structure of P450s was the removal of the trans-membrane domain of P450s. It has to be admitted that there are many limitations for the common use of crystal structures of the soluble domains of P450s in understanding the mechanism of drug metabolism. Recent studies about the structures of membrane-bound cytochrome P450 complex [50–52] have provided solid foundation to explore the influence of the lipid membrane on the function of P450 [53]. It has been suggested that anchorage of the proteins in a lipid bilayer is a minimal requirement for P450s catalytic function, which leads to more efficient transfer of electrons from P450s redox partners, e.g., cyt b5 and CYP450-reductase (CPR) [51, 52]. In addition, lipid membrane can induce conformational changes in the fl-FBD-P450s complex, which contribute to the higher affinity between the redox partners [54]. Moreover, the membrane environment can modulate the changes in the spin multiplicity equilibrium of the heme, which may be related to the heme solvent exposure [49]. Furthermore, the lipophilic substrates likely participate in the P450s-mediated reaction via the hydrophobic core of the lipid membrane rather than the cytosol. The “hydrophobic channel” exposed to leaf of membrane plays an essential role in the migration of ligands to the active site [55]. Thus, in the membrane environment, the introduction of substrate not only can affect the dynamic interplay between P450s and redox partners greatly, but also can alter the spin state of heme iron. With the recent finding of the important role of the membrane and local lipid heterogeneity on P450's structure and function [56], it is not enough to understand the metabolic mechanism only considering the soluble domain of P450s. Therefore, in the near future, we will put more effort to explore the drug metabolism mediated by P450s in the membrane environment.

## Conclusions

In summary, on the basis of the DFT computational result, we found that 2,5-diaminothiophene, the thiophenes-containing molecule, can be bioactivated into 2,5-diimine thiophene-reactive intermediate by Cpd I through the successive abstraction of two hydrogen atoms. Regio-selectivity occurred during the abstraction of the first H atom as a result of the self-controlled conformational turn to deposit the second H atom near the porphyrin. The second hydrogen was abstracted through a proton-shuttle mechanism via the formation of porphyrin *N*-protonated complex in HS state. This reaction path was preferred in HS because the energy barrier in HS was much lower than that in LS in protein



environment. With the discovery of such a mechanism, we can know that molecules with such a bioactivation mechanism will not be suitable to use structure-based methods to predict the regio-selectivity. Also it will help us to avoid the occurrence of bioactivation in rational design of thiophene-contained drugs.

Tables S1–S7, Figures S1–S10, and Cartesian coordinates of the geometries discussed in the context were shown in the Supplementary file.

**Acknowledgements** This work was supported by the China Postdoctoral Science Foundation (Grant no. 2017M622784), the National Natural Science Foundation of China (Grant no. 81173124), Shenzhen Science and Technology Innovation Commission (Grant nos. JCYJ20160308104109234 and KQJSCX20170728150303243), and the National Key Research and Development Program of China (Grant no. 2017YFC1702006).

## References

- Baskaran UL, Sabina EP (2017) Clinical and experimental research in antituberculosis drug-induced hepatotoxicity: a review. *J Integr Med-Jim* 15(1):27–36. [https://doi.org/10.1016/s2095-4964\(17\)60319-4](https://doi.org/10.1016/s2095-4964(17)60319-4)
- Kullak-Ublick GA, Andrade RJ, Merz M, End P, Benesic A, Gerbes AL, Aithal GP (2017) Drug-induced liver injury: recent advances in diagnosis and risk assessment. *Gut* 66(6):1154–1164. <https://doi.org/10.1136/gutjnl-2016-313369>
- Fontana RJ (2014) Pathogenesis of idiosyncratic drug-induced liver injury and clinical perspectives. *Gastroenterology* 146(4):914–U437. <https://doi.org/10.1053/j.gastro.2013.12.032>
- Fang Z-Z, Zhang Y-Y, Wang X-L, Cao Y-F, Huo H, Yang L (2011) Bioactivation of herbal constituents: simple alerts in the complex system. *Expert Opin Drug Metab Toxicol* 7(8):989–1007. <https://doi.org/10.1517/17425255.2011.586335>
- Guengerich FP (2003) Cytochrome P450 oxidations in the generation of reactive electrophiles: epoxidation and related reactions. *Arch Biochem Biophys* 409(1):59–71
- Guengerich FP (2008) Cytochrome P450 and chemical toxicology. *Chem Res Toxicol* 21(1):70–83. <https://doi.org/10.1021/tx700079z>
- Dekant W (2009) The role of biotransformation and bioactivation in toxicity. In: Luch A (eds) *Molecular, clinical and environmental toxicology. Experientia Supplementum*, vol 99. Springer, Basel, Boston, Berlin, Germany
- Brewer CT, Chen TS (2017) Hepatotoxicity of herbal supplements mediated by modulation of cytochrome P450. *Int J Mol Sci*. <https://doi.org/10.3390/ijms18112353>
- Hollenberg PF, Kent UM, Bumpus NN (2008) Mechanism-based inactivation of human cytochromes P450s: experimental characterization, reactive intermediates, and clinical implications. *Chem Res Toxicol* 21(1):189–205. <https://doi.org/10.1021/tx7002504>
- Dalvie DK, Kalgutkar AS, Khojasteh-Bakht SC, Obach RS, O'Donnell JP (2002) Biotransformation reactions of five-membered aromatic heterocyclic rings. *Chem Res Toxicol* 15(3):269–299. <https://doi.org/10.1021/tx015574b>
- Stepan AF, Walker DP, Bauman J, Price DA, Baillie TA, Kalgutkar AS, Aleo MD (2011) Structural alert/reactive metabolite concept as applied in medicinal chemistry to mitigate the risk of idiosyncratic drug toxicity: a perspective based on the critical examination of trends in the top 200 drugs marketed in the United States. *Chem Res Toxicol* 24(9):1345–1410. <https://doi.org/10.1021/tx200168d>
- Le Dang N, Hughes TB, Miller GP, Swamidass J (2017) Computational approach to structural alerts: furans, phenols, nitroaromatics, and thiophenes. *Chem Res Toxicol* 30(4):1046–1059. <https://doi.org/10.1021/acs.chemrestox.6b00336>
- Gramac D, Masic LP, Dolenc MS (2014) Bioactivation potential of thiophene-containing drugs. *Chem Res Toxicol* 27(8):1344–1358. <https://doi.org/10.1021/tx500134g>
- Chan GFQ, Towers GHN, Mitchell JC (1975) Ultraviolet-mediated antibiotic activity of thiophene compounds of targetes. *Phytochemistry* 14(10):2295–2296. [https://doi.org/10.1016/s0031-9422\(00\)91121-x](https://doi.org/10.1016/s0031-9422(00)91121-x)
- Hudson JB, Graham EA, Miki N, Towers GHN, Hudson LL, Rossi R, Carpita A, Neri D (1989) Photoactive antiviral and cytotoxic activities of synthetic thiophenes and their acetylenic derivatives. *Chemosphere* 19(8–9):1329–1343. [https://doi.org/10.1016/0045-6535\(89\)90080-5](https://doi.org/10.1016/0045-6535(89)90080-5)
- Matsuura H, Saxena G, Farmer SW, Hancock REW, Towers GHN (1996) Antibacterial and antifungal polyine compounds from *Glehnia littoralis* ssp *leiocarpa*. *Planta Med* 62(3):256–259. <https://doi.org/10.1055/s-2006-957872>
- Lecoeur S, Andre C, Beaune PH (1996) Tienilic acid-induced autoimmune hepatitis: anti-liver and -kidney microsomal type 2 autoantibodies recognize a three-site conformational epitope on cytochrome P4502C9. *Mol Pharmacol* 50(2):326–333
- Mansuy D (1997) Molecular structure and hepatotoxicity: compared data about two closely related thiophene compounds. *J Hepatol* 26:22–25. [https://doi.org/10.1016/s0168-8278\(97\)80493-x](https://doi.org/10.1016/s0168-8278(97)80493-x)
- Niemegeers CJ, Lenaerts FM, Awouters F, Janssen PAJ (1975) Gastrointestinal effects and acute toxicity of suprofen. *Arzneimittel-Forsch/Drug Res* 25(10):1537–1542
- Castell JV, Gomezlechon MJ, Grassa C, Martinez LA, Miranda MA, Tarrega P (1994) Photodynamic lipid-peroxidation by the photosensitizing nonsteroidal antiinflammatory drugs suprofen and tiaprofenic acid. *Photochem Photobiol* 59(1):35–39. <https://doi.org/10.1111/j.1751-1097.1994.tb04998.x>
- Priestley CC, Regan S, Park BK, Williams DP (2011) The genotoxic potential of methapyrilene using the alkaline Comet assay in vitro and in vivo. *Toxicology* 290(2–3):249–257. <https://doi.org/10.1016/j.tox.2011.10.002>
- Mercer AE, Regan SL, Hirst CM, Graham EE, Antoine DJ, Benson CA, Williams DP, Foster J, Kenna JG, Park BK (2009) Functional and toxicological consequences of metabolic bioactivation of methapyrilene via thiophene S-oxidation: induction of cell defence, apoptosis and hepatic necrosis. *Toxicol Appl Pharmacol* 239(3):297–305. <https://doi.org/10.1016/j.taap.2009.05.027>
- Hutzler JM, Balogh LM, Zientek M, Kumar V, Tracy TS (2009) Mechanism-based inactivation of cytochrome P450 2C9 by tienilic acid and (±)-suprofen: a comparison of kinetics and probe substrate selection. *Drug Metab Dispos* 37(1):59–65. <https://doi.org/10.1124/dmd.108.023358>
- Rademacher PM, Woods CM, Huang Q, Szklarz GD, Nelson SD (2012) Differential oxidation of two thiophene-containing regioisomers to reactive metabolites by cytochrome P450 2C9. *Chem Res Toxicol* 25(4):895–903. <https://doi.org/10.1021/tx200519d>
- Dansette PM, Bertho G, Mansuy D (2005) First evidence that cytochrome P450 may catalyze both S-oxidation and epoxidation of thiophene derivatives. *Biochem Biophys Res Commun* 338(1):450–455. <https://doi.org/10.1016/j.bbrc.2005.08.091>
- Mansuy D, Dansette PM (2011) Sulfenic acids as reactive intermediates in xenobiotic metabolism. *Arch Biochem Biophys* 507(1):174–185. <https://doi.org/10.1016/j.abb.2010.09.015>

27. Dansette PM, Thang DC, Elamri H, Mansuy D (1992) Evidence for thiophene-*s*-oxide as a primary reactive metabolite of thiophene *in vivo*—formation of a dihydrothiophene sulfoxide mercapturic acid. *Biochem Biophys Res Commun* 186(3):1624–1630. [https://doi.org/10.1016/s0006-291x\(05\)81594-3](https://doi.org/10.1016/s0006-291x(05)81594-3)
28. Hu Y, Yang S, Shilliday FB, Heyde BR, Mandrell KM, Robins RH, Xie J, Reding MT, Lai Y, Thompson DC (2010) novel metabolic bioactivation mechanism for a series of anti-inflammatory agents (2,5-diaminothiophene derivatives) mediated by cytochrome P450 enzymes. *Drug Metab Dispos* 38(9):1522–1531. <https://doi.org/10.1124/dmd.110.032581>
29. Kumar D, de Visser SP, Sharma PK, Cohen S, Shaik S (2004) Radical clock substrates, their C–H hydroxylation mechanism by cytochrome P450, and other reactivity patterns: What does theory reveal about the clocks' behavior? *J Am Chem Soc* 126(6):1907–1920. <https://doi.org/10.1021/ja039439s>
30. de Visser SP, Shaik S (2003) A proton-shuttle mechanism mediated by the porphyrin in benzene hydroxylation by cytochrome P450 enzymes. *J Am Chem Soc* 125(24):7413–7424. <https://doi.org/10.1021/ja034142f>
31. de Visser SP, Kumar D, Cohen S, Shacham R, Shaik S (2004) A predictive pattern of computed barriers for C–H hydroxylation by compound I of cytochrome P450. *J Am Chem Soc* 126(27):8362–8363. <https://doi.org/10.1021/ja04858h>
32. Cohen S, Kozuch S, Hazan C, Shaik S (2006) Does substrate oxidation determine the regioselectivity of cyclohexene and propene oxidation by cytochrome P450? *J Am Chem Soc* 128(34):11028–11029. <https://doi.org/10.1021/ja063269c>
33. Mallick D, Shaik S (2017) Kinetic isotope effect probes the reactive Spin state, as well as the geometric feature and constitution of the transition State during H-abstraction by heme compound II complexes. *J Am Chem Soc* 139(33):11451–11459. <https://doi.org/10.1021/jacs.7b04247>
34. de Visser SP, Ogliaro F, Sharma PK, Shaik S (2002) What factors affect the regioselectivity of oxidation by cytochrome P450? A DFT study of allylic hydroxylation and double bond epoxidation in a model reaction. *J Am Chem Soc* 124(39):11809–11826. <https://doi.org/10.1021/ja026872d>
35. Bathelt CM, Ridder L, Mulholland AJ, Harvey JN (2003) Aromatic hydroxylation by cytochrome P450: model calculations of mechanism and substituent effects. *J Am Chem Soc* 125(49):15004–15005. <https://doi.org/10.1021/ja035590q>
36. Ai C-Z, Liu Y, Li W, Chen D-M, Zhu X-X, Yan Y-W, Chen D-C, Jiang Y-Z (2017) Computational explanation for bioactivation mechanism of targeted anticancer agents mediated by cytochrome P450s: a case of erlotinib. *Plos One* 12(6):1. <https://doi.org/10.1371/journal.pone.0179333>
37. Shaik S, Kumar D, de Visser SP, Altun A, Thiel W (2005) Theoretical perspective on the structure and mechanism of cytochrome P450 enzymes. *Chem Rev* 105(6):2279–2328. <https://doi.org/10.1021/cr030722j>
38. Schyman P, Lai W, Chen H, Wang Y, Shaik S (2011) The directive of the protein: how does cytochrome P450 select the mechanism of dopamine formation? *J Am Chem Soc* 133(20):7977–7984. <https://doi.org/10.1021/ja201665x>
39. Mulliken RS (1955) Electronic population analysis on LCAO-MO molecular wave functions. 3. Effects of hybridization on overlap and gross Ao populations. *Journal of Chemical Physics* 23(12):2338–2342. <https://doi.org/10.1063/1.1741876>
40. de Visser SP, Ogliaro F, Harris N, Shaik S (2001) Multi-state epoxidation of ethene by cytochrome P450: a quantum chemical study. *J Am Chem Soc* 123(13):3037–3047
41. Harris DL, Loew GH (1998) Theoretical investigation of the proton assisted pathway to formation of cytochrome P450 compound I. *J Am Chem Soc* 120(35):8941–8948. <https://doi.org/10.1021/ja981059x>
42. Schoneboom JC, Lin H, Reuter N, Thiel W, Cohen S, Ogliaro F, Shaik S (2002) The elusive oxidant species of cytochrome P450 enzymes: characterization by combined quantum mechanical/molecular mechanical (QM/MM) calculations. *J Am Chem Soc* 124(27):8142–8151. <https://doi.org/10.1021/ja026279w>
43. Frisch MJ, Trucks GW, Schlegel HB, Scuseria GE, Robb MA, Cheeseman JR, Scalmani G, Barone V, Mennucci B, Petersson GA, Nakatsuji H, Caricato M, Li X, Hratchian HP, Izmaylov AF, Bloino J, Zheng G, Sonnenberg JL, Hada M, Ehara M, Toyota K, Fukuda R, Hasegawa J, Ishida M, Nakajima T, Honda Y, Kitao O, Nakai H, Vreven T, Montgomery JA Jr., Peralta JE, Ogliaro F, Bearpark M, Heyd JJ, Brothers E, Kudin KN, Staroverov VN, Kobayashi R, Normand J, Raghavachari K, Rendell A, Burant JC, Iyengar SS, Tomasi J, Cossi M, Rega N, Millam JM, Klene M, Knox JE, Cross JB, Bakken V, Adamo C, Jaramillo J, Gomperts R, Stratmann RE, Yazyev O, Austin AJ, Cammi R, Pomelli C, Ochterski JW, Martin RL, Morokuma K, Zakrzewski VG, Voth GA, Salvador P, Dannenberg JJ, Dapprich S, Daniels AD, Farkas Ö, Foresman JB, Ortiz JV, Cioslowski J, Fox DJ (2009) Gaussian 09, Revision D.01. Gaussian, Inc., Wallingford CT
44. Hirao H, Chuanprasit P, Cheong YY, Wang X (2013) How is a metabolic intermediate formed in the mechanism-based inactivation of cytochrome P450 by using 1,1-dimethylhydrazine: hydrogen abstraction or nitrogen oxidation? *Chemistry-a Eur J* 19(23):7361–7369. <https://doi.org/10.1002/chem.201300689>
45. Sevrioukova IF, Poulos TL (2017) Structural basis for regio-specific midazolam oxidation by human cytochrome P450 3A4. *Proc Natl Acad Sci USA* 114(3):486–491. <https://doi.org/10.1073/pnas.1616198114>
46. Ogliaro F, Cohen S, Filatov M, Harris N, Shaik S (2000) The high-valent compound of cytochrome P450: The nature of the Fe-S bond and the role of the thiolate ligand as an internal electron donor. *Angew Chemie-Int Edit* 39(21):3851. [https://doi.org/10.1002/1521-3773\(20001103\)39:21%3c3851:aid-anie3851%3e3.0.co;2-9](https://doi.org/10.1002/1521-3773(20001103)39:21%3c3851:aid-anie3851%3e3.0.co;2-9)
47. Kumar D, de Visser SP, Shaik S (2003) How does product isotope effect prove the operation of a two-state “rebound” mechanism in C–H hydroxylation by cytochrome P450? *J Am Chem Soc* 125(43):13024–13025. <https://doi.org/10.1021/ja036906x>
48. Ji L, Schueuermann G (2013) Model and mechanism: *N*-hydroxylation of primary aromatic amines by cytochrome P450. *Angew Chemie-Int Edit* 52(2):744–748. <https://doi.org/10.1002/anie.201204116>
49. Ravula T, Barnaba C, Mahajan M, Anantharamaiah GM, Im S-C, Waskell L, Ramamoorthy A (2017) Membrane environment drives cytochrome P450's spin transition and its interaction with cytochrome b(5). *Chem Commun* 53(95):12798–12801. <https://doi.org/10.1039/c7cc07520k>
50. Ahuja S, Jahr N, Im SC, Vivekanandan S, Popovych N, Le Clair SV, Huang R, Soong R, Xu JD, Yamamoto K, Nanga RP, Bridges A, Waskell L, Ramamoorthy A (2013) A model of the membrane-bound cytochrome b(5)-Cytochrome P450 complex from NMR and mutagenesis data. *J Biol Chem* 288(30):22080–22095. <https://doi.org/10.1074/jbc.M112.448225>
51. Zhang M, Huang R, Im SC, Waskell L, Ramamoorthy A (2015) Effects of membrane mimetics on cytochrome P450-Cytochrome b(5) interactions characterized by NMR spectroscopy. *J Biol Chem* 290(20):12705–12718. <https://doi.org/10.1074/jbc.M114.597096>
52. Prade E, Mahajan M, Im SC, Zhang M, Gentry KA, Anantharamaiah GM, Waskell L, Ramamoorthy A (2018) A minimal functional complex of cytochrome P450 and FBD of cytochrome P450 reductase in nanodiscs. *Angew Chemie-Int Edit* 57(28):8458–8462. <https://doi.org/10.1002/anie.201802210>

53. Denisov IG, Sligar SG (2016) Nanodiscs for structural and functional studies of membrane proteins. *Nat Struct Mol Biol* 23(6):481–486. <https://doi.org/10.1038/nsmb.3195>
54. Mahajan M, Ravula T, Prade E, Anantharamaiah GM, Ramamoorthy A (2019) Probing membrane enhanced protein-protein interactions in a minimal redox complex of cytochrome-P450 and P450-reductase. *Chem Commun (Camb, Engl)* 55(41):1. <https://doi.org/10.1039/c9cc01630a>
55. Barnaba C, Ramamoorthy A (2018) Picturing the membrane-assisted choreography of cytochrome P450 with lipid nanodiscs. *Chem Phys Chem* 19(20):2603–2613. <https://doi.org/10.1002/cphc.201800444>
56. Hollingsworth SA, Batabyal D, Nguyen BD, Poulos TL (2016) Conformational selectivity in cytochrome P450 redox partner interactions. *Proc Natl Acad Sci USA* 113(31):8723–8728. <https://doi.org/10.1073/pnas.1606474113>

**Publisher's Note** Springer Nature remains neutral with regard to jurisdictional claims in published maps and institutional affiliations.